Fabrication and characterization of the modified ev31-based metal matrix nanocomposites

metals

MDPI

Article

Fabrication and Characterization of the Modified EV31-Based Metal Matrix Nanocomposites

Seyed Kiomars Moheimani [1,2,*], Mehran Dadkhah [3], Mohammad Hossein Mosallanejad [4] and Abdollah Saboori [3]

[1] Advanced Materials Research Center, Department of Materials Engineering, Islamic Azad University, Najaf Abad Branch, Najaf Aba 8514143131, Iran
[2] Department of Research and Development, Nejat Darya Co., Bushehr 7513898849, Iran
[3] Department of Applied Science and Technology, Politecnico di Torino, Corso Duca Degli Abruzzi 24, 10129 Torino, Italy; mehran.dadkhah@polito.it (M.D.); abdollah.saboori@polito.it (A.S.)
[4] Department of Materials Engineering, Isfahan University of Technology, Isfahan 8415683111, Iran; Mh.mosallanejad@studenti.polito.it
* Correspondence: moheimani@amconsult.com.au; Tel.: +61-421164494

Abstract: Metal matrix nanocomposites (MMNCs) with high specific strength have been of interest for numerous researchers. In the current study, Mg matrix nanocomposites reinforced with AlN nanoparticles were produced using the mechanical stirring-assisted casting method. Microstructure, hardness, physical, thermal and electrical properties of the produced composites were characterized in this work. According to the microstructural evaluations, the ceramic nanoparticles were uniformly dispersed within the matrix by applying a mechanical stirring. At higher AlN contents, however, some agglomerates were observed as a consequence of a particle-pushing mechanism during the solidification. Microhardness results showed a slight improvement in the mechanical strength of the nanocomposites following the addition of AlN nanoparticles. Interestingly, nanocomposite samples were featured with higher electrical and thermal conductivities, which can be attributed to the structural effect of nanoparticles within the matrix. Moreover, thermal expansion analysis of the nanocomposites indicated that the presence of nanoparticles lowered the Coefficient of Thermal Expansion (CTE) in the case of nanocomposites. All in all, this combination of properties, including high mechanical strength, thermal and electrical conductivity, together with low CTE, make these new nanocomposites very promising materials for electro packaging applications.

Keywords: metal matrix nanocomposite; casting; thermophysical properties; coefficient of thermal expansion

Citation: Moheimani, S.K.; Dadkhah, M.; Mosallanejad, M.H.; Saboori, A. Fabrication and Characterization of the Modified EV31-Based Metal Matrix Nanocomposites. *Metals* **2021**, *11*, 125. https://doi.org/10.3390/met11010125

Received: 8 December 2020
Accepted: 8 January 2021
Published: 10 January 2021

1. Introduction

In recent years, various studies have assessed the incorporation of nano-sized particles (as reinforcement) in metal matrix composites due to their unique characteristics [1–6]. The mechanical properties of conventional alloys including, strength, fatigue, stiffness and creep resistance, as well as physical and chemical features, could be significantly improved by the addition of nano-sized particles to a metal matrix [7–10]. Among the MMCs, the existing literature on magnesium matrix composites is extensive and focuses particularly on their applications in modern industries [11–16]. In fact, the low density of magnesium, compared to aluminium and steel, and its strength/ductility ratio make it a suitable option in various applications such as automotive, aerospace and electronics [17,18]. Moreover, improvement of mechanical properties by heat treatment of complex as-cast parts is a time-consuming process and even sometimes becomes impossible [19]. Good castability and fine microstructure are significant factors that should be taken into account in designing a castable alloy with lightweight. A common method fulfilling the above goals is the production of MMCs by homogeneous incorporation of nanoparticles in

the molten alloy. On the other hand, the applications of lightweight Mg and its alloys, particularly at high temperatures, are faced with limitations due to their scarce creep behaviour, relatively low strength and modulus. Therefore, efforts have recently been paid to the use of magnesium alloys for high-temperature applications, e.g., gearbox casings for the helicopter industry [20], which led to the development of Mg–rare earth (RE) alloys with superior mechanical characteristics both at room and high temperatures [21,22]. Actually, the addition of rare earth elements is an important factor for achieving thermal stability of microstructure, creep and mechanical properties of magnesium alloys. One of the recently developed commercial alloys of magnesium is EV3, formerly known as Elektron21, which is widely used for high-temperature applications (up to 200 °C) and contains Nd, Gd, Zn and Zr elements. In magnesium alloys, Nd, with a low solid solubility limit, enhances the strength, especially at high temperatures. Gd, on the other hand, presents a reduced solid solubility at low temperatures, leading to the improvement of the precipitation-strengthening effect [18,23]. Lyon et al. [18] reported the enhancement of the castability in terms of micro-shrinkage, as a result of adding both gadolinium and neodymium. The addition of a small amount of zinc (up to 1.3%) increases mechanical strength improvement with no ductility reduction. Furthermore, a fine-grained structure was obtained in the presence of zirconium which resulted in improvement of mechanical features, castability and corrosion resistance of Mg [23].

Besides the mechanical features at high temperatures, thermal properties, including thermal conductivity and specific heat capacity, are important driving factors in high-temperature applications [17,24]. Therefore, the mechanical and thermal characteristics of Mg-based composites should be precisely determined for high-temperature applications. Up to now, few data have been reported regarding the thermal properties of EV31. Kiełbus et al. [24] studied the thermal diffusivity of WE54 and Elektron21 Magnesium alloys and reported correlations between temperature, microstructure and the thermal diffusivity. Elektron21 was described as having a better thermal conductivity as compared to the WE54, thanks to the lower amount of solutes in the Elektron21 alloy. The authors further addressed the effect of ageing treatment and found improved thermal conductivity as a result of heat treatment. Formation of more precipitates in Elektron21 after the heat treatment, accompanied by consumption of more solutes, improved the thermal conductivity of the alloy [24]. Carseten et al. [25] produced Mg90Ni10-ENG composites by compressing a mixed blend of Mg90Ni10 and ENG. The results by the author showed the composite thermal conductivity could be tuned in a wide range by controlling the amount of the second phase material, i.e., graphite. Tani et al. [26] addressed the thermoelectric properties of Mg_2Si-based in situ composites produced by a reduction process. They reported a dimensionless thermoelectric figure of merit (ZT) as being influenced by the additive used. Moreover, Saboori et al. [19] produced Elektron21 composites reinforced by AlN nanoparticles. They investigated the electrical conductivity of the samples in a wide temperature range and reported a significant change in the thermal and electrical properties, citing the formation of Al_2Nd as a result of the introduced nanoparticles [16]. However, microstructure, thermophysical and mechanical performance of a modified EV31 has never been studied. In fact, addition of Al as an alloying element is supposed to be very effective for the thermophysical properties and improved the electrical and thermal conductivity of the modified alloy and its composites. Therefore, the aim of this paper is to analyse the effect of Al (as an alloying element) and AlN (as a reinforcement) addition on the microstructure and thermophysical properties of EV31. For this reason, the thermal and electrical properties of these composites, together with their phase changes and the consequent influences on the CTE and their microhardness, were investigated.

2. Materials and Methods

Commercial EV31 with the composition shown in Table 1 was melted in a vacuum resistance furnace (YMVR 1500, Tehran, Iran) equipped with a graphite crucible. Prior to casting, the graphite crucible was heated up to 900 °C in a furnace to remove the

contaminations from the surface of the crucible and then cooled down to the ambient temperature and washed using NaOH. Afterwards, the melt was superheated up to 730 °C and kept at this temperature for 45 min and then poured into a preheated cylindrical carbon steel mould. In the case of Metal matrix nanocomposites (MMNCs), before the casting, AlN nanopowder (<100 nm) supplied by Merck were added together with 0.1% aluminium in the form of a master alloy and dispersed into the molten EV31 through the mechanical stirring method for 10 min (200 rpm). Subsequently, the mould containing molten alloy was quickly cooled down by using a water bath to avoid the sedimentation of nanoparticles.

Table 1. Chemical composition of the starting alloy.

Chemical Composition	Nd	Gd	Zn	Zr	Al	Mg
Standard (Wt.%)	2.6–3.1	1.0–1.7	0.2–0.5	Saturated	-	Bal.
Nominal (wt.%)	2.9	1.3	0.4	0.4	0.1	Bal.

Optical microscope (OM, Olympus, Tokyo, Japan) and scanning electron microscope (SEM, TESCAN, Kohoutovice, Czech Republic) was used to study the microstructure of specimens. The samples were mounted in resin and then ground with SiC papers down to 4000 grit size and thereafter by diamond paste (down to 1 µm). Finally, the polished cross-section of the samples was etched using a 9% picric acid solution. A tabletop scanning electron microscope (SEM; Hitachi, Tokyo, Japan, operating at 15 kV) equipped with an energy-dispersive X-ray spectrometer (EDS, Munich, Germany) was employed for chemical and microstructural evaluations. The line-intercept method was used to calculate the grain size of the matrix and MMNCs. X-ray diffraction (XRD) patterns of as-polished samples were investigated using a Philips X'Pert Diffractometer (Philips, Almelo, The Netherland) using Cu-Kα radiation. Hardness measurements were carried out on as polished surfaces with a load of 5 kg with a dwell time of 15 s. The reported hardness results are the average of five measurements per sample. In order to evaluate the electrical conductivity, the electrical resistivity of the specimens was measured and then converted to the electrical conductivity feature. The room temperature thermal conductivity of the specimens was measured using the Transient Plane Source (TPS) method. Thermal expansion of the MMNCs in the range of 25–450 °C was evaluated by a SETSYS Evolution TMA (Setaram Instrumentation, Caluir, France) using 5 °C/min as the heating rate and argon as the protective atmosphere. For this reason, cylindrical samples with a dimension of ϕ5 mm × 120 mm were machined from the as-cast billets. Prior to the analysis, the TMA apparatus was calibrated according to DIN 51045 with NBS-Pt.

3. Results and Discussion

Figure 1a shows the optical micrograph of the as-cast modified EV31, which consisted of α-Mg solid solution and Mg_3(Nd,Gd) eutectic phases on the grain boundaries. In fact, Mg_3Nd is modified as Mg_3(Nd,Gd) eutectic phase by partial substitution of Nd with Gd without altering the crystal structure. Actually, due to the negligible differences between the atomic radii of Nd and Gd, this replacement does distort the crystal structure [24]. Moreover, the simultaneous presence of Gd and Nd in the eutectic phase is confirmed by EDS-map analysis of as-cast EV31, as can be seen in Figure 2. In addition, the incorporation of AlN nanoparticles led to a slight gain refinement as shown by the average grain measurement, which is carried out by image analysis. As shown in Figure 1, by addition of 1% and 2% AlN, the average grain size of the modified EV31 (78.5 µm) is decreased to 70.6 and 68.8 µm, respectively. From Figure 1b, it can be seen that despite the presence of some agglomeration, AlN nanoparticles are rather homogeneously dispersed in as-cast modified EV31-2%AlN.

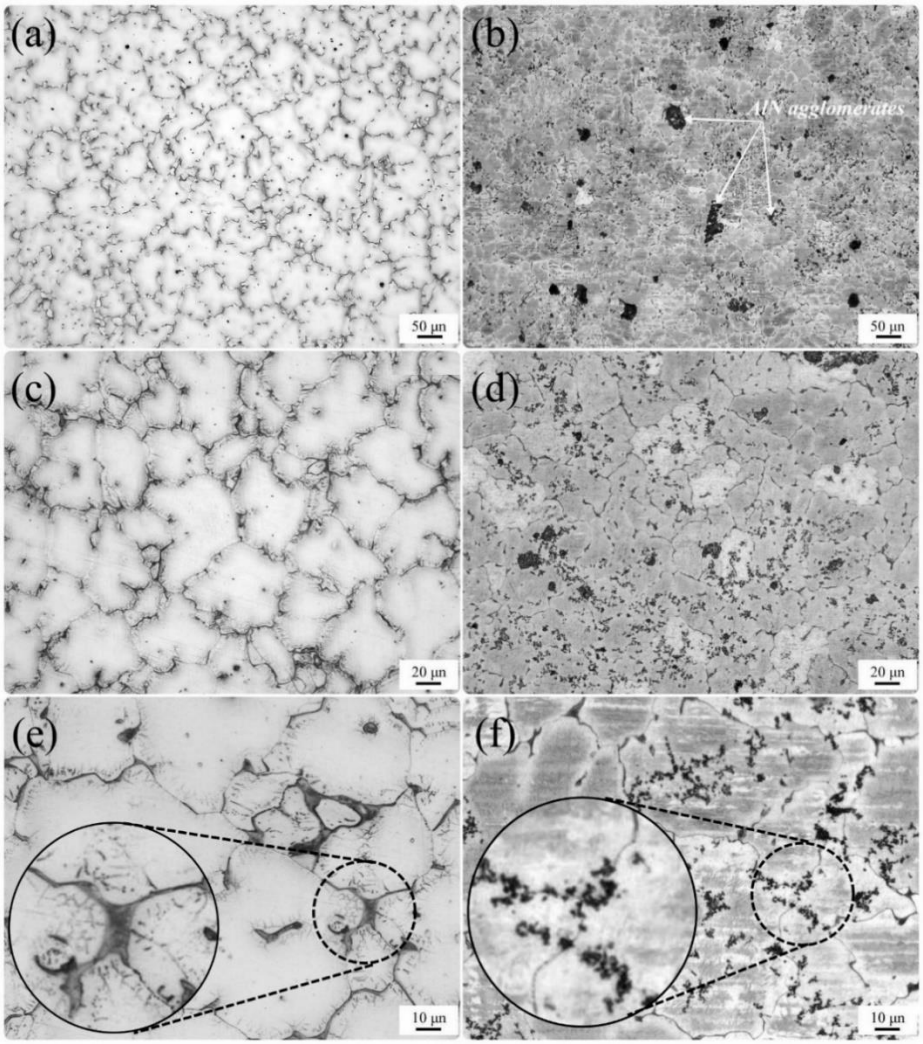

Figure 1. Optical micrograph of (**a**,**c**,**e**) as-cast modified EV31, (**b**,**d**,**f**) as-cast modified EV31-2%AlN.

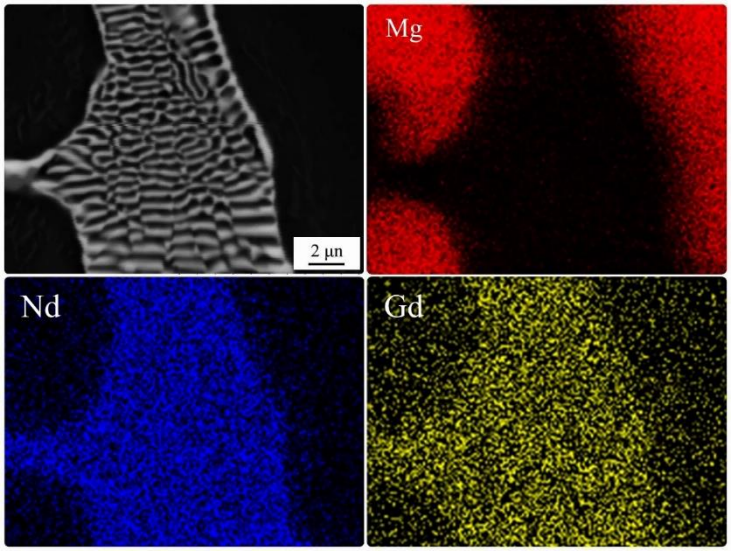

Figure 2. EDS-map analysis of as-cast modified EV31.

Figure 3 depicts the SEM images for the as-cast modified EV31 along with the SEM image of the modified EV31-2%AlN sample. As mentioned earlier in this text, though AlN

agglomerates are observed in Figure 3b, there is a fairly homogenous distribution of the second phase material within the matrix. It is reported that Mg-Nd-Gd ternary diagram includes Mg_3RE intermetallic for Mg-rich compositions [27]. As compared with the as-cast sample (Figure 3a), less Mg_3RE phases are formed in the grain boundary of the α-Mg grains, a phenomenon that may be attributed to the possible reactions between the RE elements and the introduced AlN nanoparticles or Al. This finding is also verified by the XRD results for as-cast modified EV31, modified EV31-1%AlN and modified EV31-2%AlN, which are demonstrated in Figure 4.

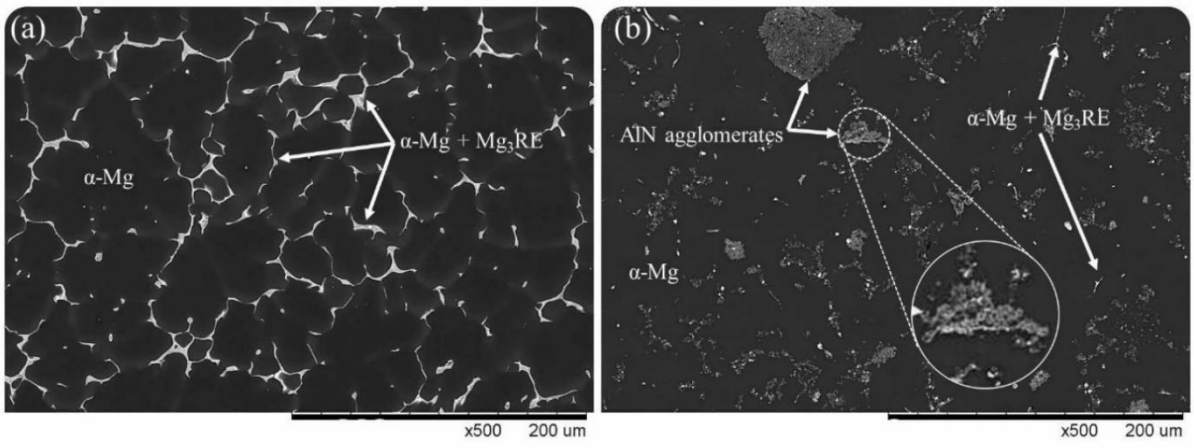

Figure 3. SEM micrographs of (**a**) as-cast modified EV31, (**b**) modified EV31-2%AlN.

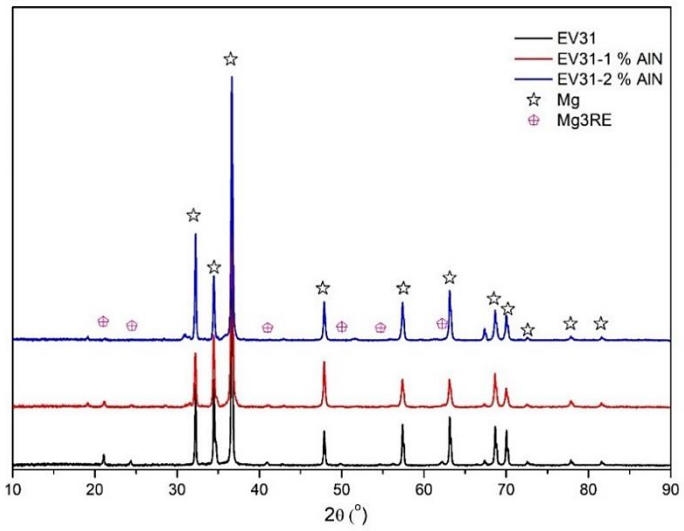

Figure 4. XRD patterns of as-cast modified EV31, modified EV31-1%AlN and modified EV31-2%AlN.

Main peaks corresponding to Mg as well as the peaks related to the Mg_3RE phase are detected as the matrix phase and the main intermetallic phase, respectively. It should be noted that a high density of intermetallic phases was observed in EV31 alloy under as-cast condition, while the addition of AlN clearly reduced the intensity of the Mg_3RE peaks. Al_2Nd peak intensity, on the other hand, follows an increasing trend with the amount of Al. Moreover, the increment in the breadth of the Mg peaks with the introduction of AlN is observed, which indicates a decrease in the matrix crystallite size. Liu et al. [28] showed that Al_2Nd particles could act as grain refiners for the α-Mg matrix. Therefore, the combined effects of the AlN and Al_2Nd particles as grain refiners can be mentioned as being influential in the matrix peak width increment.

Figure 5 shows the microhardness of the as-cast modified EV31 and its corresponding nanocomposites (modified EV31-1%AlN and modified EV31-2%AlN). It is apparent from this figure that by addition of AlN (1 and 2 wt.%), there has been a slight increase in the microhardness of modified EV31-AlN nanocomposites. The results reported in Figure 5 indicate that there is only a slight change in the hardness of the samples as a result of the AlN addition. This negligible improvement of the hardness, however, can be attributed to the dislocation motions being retarded by the AlN nanoparticles.

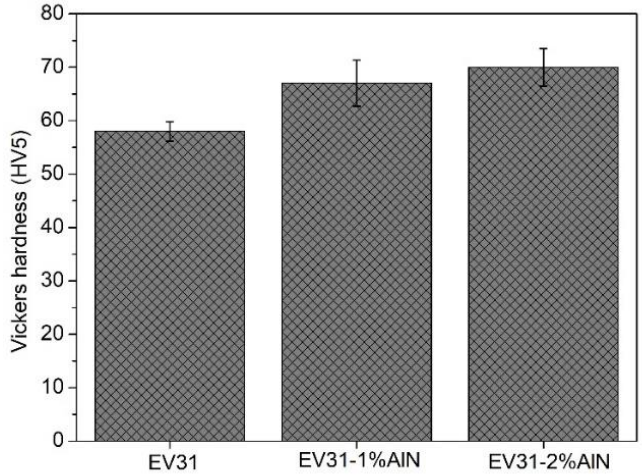

Figure 5. Vickers hardness of as-cast modified EV31, modified EV31-1%AlN and modified EV31-2%AlN.

Moreover, it should be noted that the elastic modulus of Al_2Nd 121.44 GPa is much higher than that of Mg_3RE 65.83 GPa [29] but far less than that of ZrN (245 GPa) [30]. Cheng et al. [31] found a direct correlation between the work of indentation and the elastic modulus of various materials. Therefore, it can be concluded that the reduction of Mg3RE phase upon introduction of AlN and the consequent formation of Al_2Nd and ZrN phases could contribute to the overall microhardness increase of the nanocomposites.

The thermal conductivity of as-cast modified EV31, modified EV31-1%AlN and modified EV31-2%AlN nanocomposites are presented in Table 2. As shown in this table, there is a clear trend of increase in thermal conductivity of nanocomposites by incorporating AlN nanoparticles. Actually, the improvement of thermal conductivity in the nanocomposites can be explained by two main phenomena, the first one being correlated to the AlN nanoparticles together with the Al addition, which plays a key role in thermal conductivity of nanocomposites. It is generally known that magnesium presents high thermal conductivity and high efficiency of heat dissipation [32]. Furthermore, it is reported that the solute elements in the multicomponent alloys scatter the phonon, hence affecting their contribution to thermal transfer [33]. As previously described by XRD patterns (Figure 4), Al2Nd forms in the nanocomposite due to the reaction between incorporated Al particles and Nd. This reaction, which consumes Nd solute elements, leads to the reduction of scattering point and correspondingly improvement in thermal conductivity of the nanocomposite as compared with the as-cast modified EV31. These findings are verified by previous research works [24,33]. For instance, the effect of solute elements on the thermal conductivity of magnesium has been evaluated by Kielbus et.al [24], where the thermal conductivity of El21 and WE54 (Mg-Y-Nd) was compared before and after the solution treatment. They showed that less solutes in the matrix would cause better thermal properties. Koltsov et al. [34] showed that ZrN could be formed via the following reaction:

$$Zr + AlN \rightarrow ZrN + Al \quad (1)$$

Table 2. Electrical and thermophysical properties of EV31, modified EV31 and its corresponding nanocomposites.

Material	EV31	EV31-0.1Al	EV31-0.1Al-AlN	EV31-0.1Al-2AlN
Electrical Resistivity (Ω·m)	7.46×10^{-8}	7.02×10^{-8}	5.38×10^{-8}	4.85×10^{-8}
Thermal conductivity (W/m·k)	114.8	119.7	130.8	149.5
Coefficient of Thermal Expansion (1/K)	25.8×10^{-6}	25.1×10^{-6}	24.2×10^{-6}	23.4×10^{-6}

On the other hand, according to López-Pérez et al. [35], ZrN can be formed by a reaction of Zr atoms from the matrix with the AlN surface, which can result in the release of Al, according to Equation (1). As shown previously by XRD (Figure 4), the Nd element (as a solute atom) can be consumed by released aluminium and form Al_2Nd. Accordingly, the thermal conductivity of modified EV31-AlN nanocomposites can be improved by these consecutive reactions through two mechanisms; (i) formation of a metallurgical bonding between the matrix and reinforcement and (ii) solute element consumption, which has a noticeable effect on thermal conductivity of EV31 alloys. It is apparent from Table 2 that following the addition of AlN, a significant decrease was recorded in the electrical resistivity. As a matter of fact, the solute element consumption resulted in a decrease in the scattering points of free electrons within the matrix. As mentioned earlier, incorporating the aluminium into the EV31 decreases the electrical resistivity due to the reduction in Nd content in solid solution as a consequence of the reaction between Al particles and Nd.

The Coefficient of Thermal Expansion (CTE) was further evaluated in this research. The CTE can provide useful information about both thermal expansion and generated stresses than can affect the mechanical properties of the composite and hence can be indicative of the composite thermal stability. It is seen from Table 2 that CTE is decreasing following the introduction of AlN particles. To clarify the changes, it should be mentioned that CTE of AlN reinforcement 4.5×10^{-6} K^{-1} [36] is smaller than that of EV31 matrix 25.8×10^{-6} K^{-1}. According to Kerner's model, which is close to the mixture rule, the addition of ceramic particles with low CTE to a metal matrix lowers the overall CTE of the composite [37]. Fabrication of low CTE MMCs with low reinforcement volume fraction is a great challenge, due to the limitation of reinforcement CTEs. The results of Table 2 show that CTE decreased by ~9.2% by the addition of only 2 wt.% AlN and trace amounts of excess Al. The interfacial bonding between the matrix and the reinforcement can be considered as an influential factor determining the CTE of the composites. In this work, excellent interfacial bonding created as a result of the superficial reaction between Zr (from matrix) and Al (from the reinforcement), effectively constrained the expansion of the Mg matrix. Moreover, this difference between the CTEs may cause a CTE mismatch between the matrix and the reinforcement, leading to residual stresses while cooling down to room temperature. These residual stresses may reduce the expansion of the composite upon heating, which in return lowers the CTE of the composite [36]. Adding to these, Al_2Nd is featured with a higher melting temperature (1200 °C) than Mg_3RE phase 780 °C [38], which in turn improves the thermal stability of the composites given the fact that the easy melting Mg_3RE formed in Mg grain boundary (Figure 2) would be replaced by a more resistant phase upon the incorporation of AlN particles.

4. Conclusions

In the present study, a modified magnesium alloy EV31 (as a matrix) reinforced by AlN nanoparticles were produced using the casting method. According to the Microstructural evaluations, the AlN nanoparticles were uniformly dispersed within the matrix. However, there were some AlN agglomerations after casting, which can be attributed to the particle pushing during the solidification of nanocomposites. Moreover, the results indicated that by incorporating the AlN nanoparticles, the grain size and hardness slightly decreased and increased, respectively, and less Mg3RE was formed along the matrix grain boundary. Thermal conductivity of the samples increased as a result of the matrix solutes being consumed by reacting with Al. Furthermore, this phenomenon led to a decrease in the

electrical resistance of the composites. CTE of the final composites decreased as compared with the as-cast sample. This was attributed to the low CTE of the AlN samples together with the CTE mismatch between the matrix and the secondary phases.

Author Contributions: Conceptualization, S.K.M., A.S.; investigation, S.K.M., M.D.; data curation, S.K.M., M.H.M.; writing—original draft preparation, S.K.M., M.D.; writing—review and editing, M.D., M.H.M., A.S.; supervision, A.S. All authors have read and agreed to the published version of the manuscript.

Funding: This research was funded by Nejat Darya Company (Iran).

Institutional Review Board Statement: Not applicable.

Informed Consent Statement: Not applicable.

Data Availability Statement: Not applicable.

Conflicts of Interest: The authors declare no conflict of interest.

References

1. Saboori, A.; Moheimani, S.K.; Pavese, M.; Badini, C.; Fino, P. New Nanocomposite Materials with Improved Mechanical Strength and Tailored Coefficient of Thermal Expansion for Electro-Packaging Applications. *Metals* **2017**, *7*, 536. [CrossRef]
2. Mosallanejad, M.H.; Shafyei, A.; Akhavan, S. Simultaneous co-deposition of SiC and CNT into the Ni coating. *Can. Metall. Q.* **2016**, *55*, 147–155. [CrossRef]
3. Daavari, M.; Atapour, M.; Mohedano, M.; Arrabal, R.; Matykina, E.; Taherizadeh, A. Biotribology and biocorrosion of MWCNTs-reinforced PEO coating on AZ31B Mg alloy. *Surf. Interfaces* **2020**, *22*, 100850. [CrossRef]
4. He, X.; Song, S.; Luo, X.; Liu, J.; An, L.; Bai, Y. Predicting ductility of Mg/SiCp nanocomposite under multiaxial loading conditions based on unit cell modeling. *Int. J. Mech. Sci.* **2020**, *184*, 105831. [CrossRef]
5. Chen, L.; Xu, J.; Choi, H.; Pozuelo, M.; Ma, X.; Bhowmick, S.; Yang, J.; Mathaudhu, S.; Li, X. Processing and properties of magnesium containing a dense uniform dispersion of nanoparticles. *Nature* **2015**, *528*, 539–543. [CrossRef] [PubMed]
6. Jinwang, Z.; Shebin, W.; Junyuan, Z.; Jinling, Z.; Bingshe, X. Effects of Nd on Microstructures and Mechanical Properties of AM60 Magnesium Alloy in Vacuum Melting. *Rare Met. Mater. Eng.* **2009**, *38*, 1141–1145. [CrossRef]
7. Sillekens, W.H.; Jarvis, D.J.; Vorozhtsov, A.; Bojarevics, V.; Badini, C.F.; Pavese, M.; Terzi, S.; Salvo, L.; Katsarou, L.; Dieringa, H. The ExoMet Project: EU/ESA Research on High-Performance Light-Metal Alloys and Nanocomposites. *Met. Mater. Trans. A* **2014**, *45*, 3349–3361. [CrossRef]
8. Saboori, A.; Pavese, M.; Badini, C.; Fino, P. Microstructure and Thermal Conductivity of Al–Graphene Composites Fabricated by Powder Metallurgy and Hot Rolling Techniques. *Acta Metall. Sin. Engl. Lett.* **2017**, *30*, 675–687. [CrossRef]
9. Saboori, A.; Pavese, M.; Badini, C.; Fino, P. Development of Al- and Cu-based nanocomposites reinforced by graphene nanoplatelets: Fabrication and characterization. *Front. Mater. Sci.* **2017**, *11*, 171–181. [CrossRef]
10. Saboori, A.; Pavese, M.; Badini, C.; Fino, P. A Novel Cu–GNPs Nanocomposite with Improved Thermal and Mechanical Properties. *Acta Metall. Sin. Engl. Lett.* **2018**, *31*, 148–152. [CrossRef]
11. Hu, H.; Yu, A.; Li, N.; Allison, J.E. Potential Magnesium Alloys for High Temperature Die Cast Automotive Applications: A Review. *Mater. Manuf. Proc.* **2003**, *18*, 687–717. [CrossRef]
12. Kulekci, M.K. Magnesium and its alloys applications in automotive industry. *Int. J. Adv. Manuf. Technol.* **2008**, *39*, 851–865. [CrossRef]
13. Musfirah, A.; Jaharah, A. Magnesium and Aluminum Alloys in Automotive Industry. *J. Appl. Sci. Res.* **2012**, *8*, 4865–4875.
14. Polmear, I.J. Magnesium alloys and applications. *Mater. Sci. Technol.* **1994**, *10*, 1–16. [CrossRef]
15. Barati, F.; Latifi, M.; Moayerifar, E.; Mosallanejad, M.H.; Saboori, A. Novel AM60-SiO2 Nanocomposite Produced via Ultrasound-Assisted Casting; Production and Characterization. *Materials* **2019**, *12*, 3946. [CrossRef]
16. Saboori, A.; Padovano, E.; Pavese, M.; Badini, C. Novel Magnesium Elektron21-AlN Nanocomposites Produced by Ultrasound-Assisted Casting; Microstructure, Thermal and Electrical Conductivity. *Materials* **2018**, *11*, 27. [CrossRef]
17. Dieringa, H. Properties of magnesium alloys reinforced with nanoparticles and carbon nanotubes: A review. *J. Mater. Sci.* **2011**, *46*, 289–306. [CrossRef]
18. Lyon, P.; Syed, I.; Heaney, S. Elektron 21-An aerospace magnesium alloy for sand cast and investment cast applications. *Adv. Eng. Mater.* **2007**, *9*, 793–798. [CrossRef]
19. Saboori, A.; Padovano, E.; Pavese, M.; Dieringa, H.; Badini, C. Effect of Solution Treatment on Precipitation Behaviors, Age Hardening Response and Creep Properties of Elektron21 Alloy Reinforced by AlN Nanoparticles. *Materails* **2017**, *10*, 1380. [CrossRef]
20. Luo, A.A. Magnesium casting technology for structural applications. *J. Magnes. Alloy.* **2013**, *1*, 2–22. [CrossRef]
21. Moreno, I.P.; Nandy, T.K.; Jones, J.W.; Allison, J.E.; Pollock, T.M. Microstructural stability and creep of rare-earth containing magnesium alloys. *Scr. Mater.* **2003**, *48*, 1029–1034. [CrossRef]

22. He, S.M.; Zeng, X.Q.; Peng, L.M.; Gao, X.; Nie, J.F.; Ding, W.J. Precipitation in a Mg–10Gd–3Y–0.4Zr (wt.%) alloy during isothermal ageing at 250 °C. *J. Alloy. Compd.* **2006**, *421*, 309–313. [CrossRef]
23. Kiełbus, A. Microstructure and Properties of Elektron 21 Magnesium Alloy. In *Magnesium Alloys-Design, Processing and Properties*; InTech: London, UK, 2011; Volume 4, pp. 281–296. ISBN 9789533075204.
24. Kiełbus, A.; Rzychoń, T.; Moskal, G. The Influence of Heat Treatment Parameters on the Thermal Diffusivity of WE54 and Elektron 21 Magnesium Alloys. In *Diffusion in Solids and Liquids VI. Defect and Diffusion Forum*; Trans Tech Publications Ltd.: Stafa-Zurich, Switzerland, 2011; Volume 312, pp. 489–494.
25. Pohlmann, C.; Röntzsch, L.; Kalinichenka, S.; Hutsch, T.; Kieback, B. Magnesium alloy-graphite composites with tailored heat conduction properties for hydrogen storage applications. *Int. J. Hydrogen Energy* **2010**, *35*, 12829–12836. [CrossRef]
26. Tani, J.; Kido, H. Fabrication and thermoelectric properties of Mg2Si-based composites using reduction reaction with additives. *Intermetallics* **2013**, *32*, 72–80. [CrossRef]
27. Xu, G.; Zhang, L.; Liu, L.; Du, Y.; Zhang, F.; Xu, K.; Liu, S.; Tan, M.; Jin, Z. Thermodynamic database of multi-component Mg alloys and its application to solidification and heat treatment. *J. Magnes. Alloy.* **2016**, *4*, 249–264. [CrossRef]
28. Liu, D.; Song, J.; Jiang, B.; Zeng, Y.; Wang, Q.; Jiang, Z.; Liu, B.; Huang, G.; Pan, F. Effect of Al content on microstructure and mechanical properties of as-cast Mg-5Nd alloys. *J. Alloys Compd.* **2018**, *737*, 263–270. [CrossRef]
29. Yang, H.; Zander, D.; Huang, Y.; Kainer, K.U.; Dieringa, H. Individual/synergistic effects of Al and AlN on the microstructural evolution and creep resistance of Elektron21 alloy. *Mater. Sci. Eng. A* **2020**, *777*, 139072. [CrossRef]
30. Tokarev, O.A.; Demchyshyn, A.V.; Avtonomov, G.A. The structure and mechanical properties of multilayer nanocrystalline TiN/ZrN coatings obtained by vacuum-arc deposition. *Proc. Appl. Ceramics* **2007**, *1*, 43–47. [CrossRef]
31. Cheng, Y.-T.; Cheng, C.-M. Relationships between hardness, elastic modulus, and the work of indentation. *Appl. Phys. Lett.* **1998**, *73*, 614–616. [CrossRef]
32. Xiuqing, Z.; Haowei, W.; Lihua, L.; Xinying, T.; Naiheng, M. The mechanical properties of magnesium matrix composites reinforced with (TiB2+TiC) ceramic particulates. *Mater. Lett.* **2005**, *59*, 2105–2109. [CrossRef]
33. Zhao, S.; Zheng, Z.; Huang, Z.; Dong, S.; Luo, P.; Zhang, Z.; Wang, Y. Cu matrix composites reinforced with aligned carbon nanotubes: Mechanical, electrical and thermal properties. *Mater. Sci. Eng. A* **2016**, *675*, 82–91. [CrossRef]
34. Koltsov, A. Wetting and interfacial reactivity in Ag–Zr/sintered AlN system. *Scr. Mater.* **2003**, *48*, 351–357. [CrossRef]
35. López-Pérez, W.; González-Hernández, R.; Rodríguez, M.J.A. Zirconium adsorption and incorporation on a reconstructed Al-T4 AlN(0001) surface. *J. Phys. Chem. Solids* **2013**, *74*, 1387–1391. [CrossRef]
36. Chen, J.; Bao, C.-G.; Liu, Z.-W.; Sun, B.-S.; Shu, Y.-C.; Li, Q.-K. Thermal Properties of Mg–Al/AlN Composites Fabricated by Powder Metallurgy. *Acta Metall. Sin. Engl. Lett.* **2018**, *31*, 641–649. [CrossRef]
37. Vaidya, R.U.; Chawla, K. Thermal expansion of metal-matrix composites. Compos. *Sci. Technol.* **1994**, *50*, 13–22. [CrossRef]
38. Hort, N.; Huang, Y.; Kainer, K.U. Intermetallics in Magnesium Alloys. *Adv. Eng. Mater.* **2006**, *8*, 235–240. [CrossRef]